PHYSICAL REVIEW E VOLUME 58, NUMBER 2 AUGUST 1998

Interaction of femtosecond laser pulses with ultrathin foils

A. Forsman, A. Ng, and G. Chiu
Department of Physics and Astronomy, University of British Columbia, 6224 Agricultural Road, Vancouver, British Columbia, Canada V6T 1Z1

R. M. More
Lawrence Livermore National Laboratory, Livermore, California 94550
(Received 24 July 1997; revised manuscript received 23 April 1998)

An approach for using intense femtosecond lasers to produce an equivalent idealized slab plasma of uniform electron density and temperature is described and demonstrated through numerical simulations. With a femtosecond laser as a probe, such a plasma allows the direct measurement of ac conductivity in the strongly coupled regime. It also serves as an initial value problem for the study of hot expanded states of matter. [S1063-651X(98)50808-2]

PACS number(s): 52.50.Jm, 52.25.Fi, 52.25.Rv, 52.40.Nk

Intense femtosecond (fs) lasers offer the possibility of producing high energy-density matter by coupling energy rapidly into a solid before significant hydrodynamic expansion occurs. This has led to a broad range of investigations including studies of transport properties [1–7] and x-ray spectroscopy of hot dense plasmas [8–13], high pressure shock waves [14], and liquid carbon [15]. As the coupling of fs laser radiation to a solid is governed largely by skin-depth deposition, the resulting plasma generally exhibits temperature and electron density gradients, even in the absence of expansion due to the short heating pulse or radiation pressure confinement [11]. The interpretation of laser-target coupling and other measurements requires detailed treatments of the nonuniform plasma [3,7]. Accordingly, physical parameters such as electrical conductivity cannot be measured to directly correspond to a single plasma state. There is great interest in finding an approach to using intense fs lasers to produce dense uniform plasmas. In this Rapid Communication, we present results of our calculations that show how an idealized uniform slab plasma can be produced and studied using ultrathin foils and ultrafast pump and probe lasers.

Our calculations are based on a one-dimensional Lagrangean hydrodynamic code, laser-target code (LTC), which incorporates an electromagnetic wave solver (EMS) to treat laser-matter interactions. The target and resulting plasma are described as dielectric media. Details of the code have been described elsewhere [16]. An idealized 20-fs [full width at half maximum (FWHM)], 400-nm pump pulse is normally incident on a 100-Å thick aluminum foil. The laser pulse shape is assumed to be similar to that of a 400-nm, 120-fs laser reported in a recent experiment [4]. The pulse is truncated at intensities below 10^{-6} of peak. The 20-fs pulse length is chosen to minimize plasma expansion. The 400-nm wavelength corresponds to the second harmonic of a titanium-sapphire laser. This eliminates the concern of prepulse for the irradiances of 10^{13}–10^{16} W/cm^2 used here. Normal incidence enhances coupling of the laser to the dense plasma region. The foil thickness corresponds to the scale lengths of skin-depth deposition and electron thermal conduction. Aluminum is used because of the available experimental and theoretical data on its physical properties. The resulting plasma is studied using a 260-nm, 20-fs (FWHM) probe with a pulse shape similar to that of the pump. The probe is incident normally on the front or rear side of the target. The shorter wavelength enhances its penetration through the expanded portion of the target front surface.

The results presented assume equal electron and ion temperatures due to a lack of nonequilibrium models that self-consistently treat the equation of state and transport properties over a wide parameter space. The effects of nonequilibrium will be addressed later. In our standard calculations, the quotidian equation of state (QEOS) [17] and the Lee-More (LM) dense plasma conductivity model [18], together with the Drude model, are used.

The rationale for considering the laser-heated ultrathin foil as a slab plasma can be found first by examining the electron density and temperature profiles at the end of the pump pulse (Fig. 1). At the lowest irradiance, the plasma density is most slablike and the temperature is reasonably uniform. At higher irradiances, plasma expansion becomes more noticeable but improved thermal conduction renders the plasma temperature more uniform. A further indication of the slab behavior is the relatively constant reflectivity and transmission of the probe pulse. For example, at a pump irradiance of 10^{15} W/cm^2, the reflectivity and transmission of the probe change from 49.5% and 12.9%, respectively, to 54.0% and 11.8% when the pump-probe delay is varied from 60 to 120 fs.

The method used to quantify the idealized slab plasma behavior of the femtosecond-laser heated ultrathin foil is as follows. First, we perform a full hydrodynamic simulation of the interaction of the pump laser with the target to yield the reflectivity R and transmission T of the pump pulse. The hydrodynamic calculation is carried through to the entire probe pulse. The peak-to-peak delay of the probe pulse is 62 fs, which corresponds to the time when 99.999% of the pump pulse energy is incident on the target. A comparison of the reflectivities $\{R_F, R_R\}$and transmission $\{T_F, T_R\}$ of front- and rear-side probes provides an assessment of the axial symmetry of the plasma. Next, we use the calculated R and T to determine energy deposition by the pump laser in the foil. Assuming that the heated foil behaves as a uniform slab at

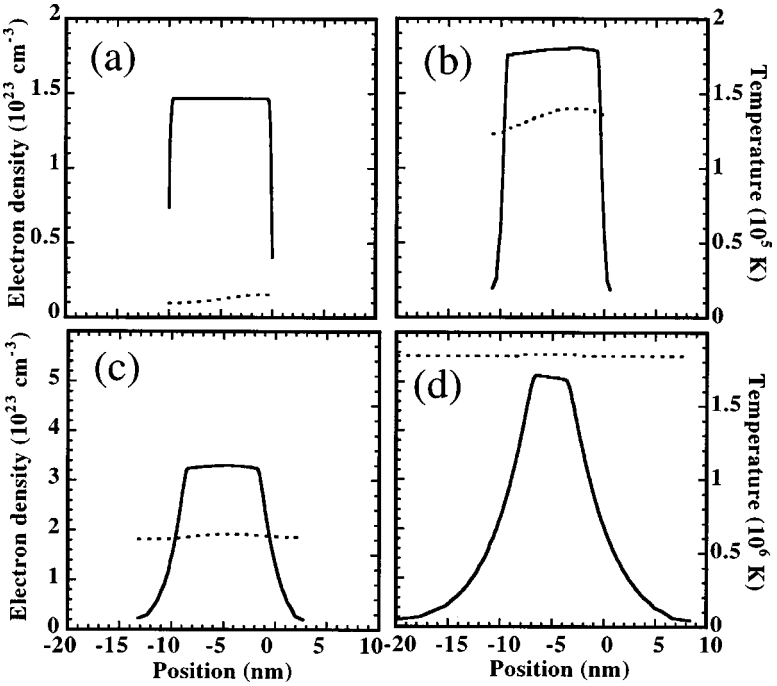

FIG. 1. Electron density (solid line) and temperature (dotted line) profiles at the end of the pump laser pulse at irradiances of (a) 10^{13} W/cm^2, (b) 10^{14} W/cm^2, (c) 10^{15} W/cm^2, and (d) 10^{16} W/cm^2. The pump laser is incident from the right.

solid density, we can determine the plasma density and temperature using the QEOS. The reflectivity R_S and transmission T_S for the probe pulse can then be calculated using the electromagnetic wave solver. For a more stringent test, we have treated the slab plasma as stationary during the probe pulse. The agreement of R_S and T_S with $\{R_F, R_R\}$ and $\{T_F, T_R\}$ is a measure of the validity of the slab model as shown in Fig. 2 for the entire range of irradiances considered.

We now describe how a hypothetical experiment using similar pump and probe lasers and ultrathin foils may be performed and interpreted. First, the reflectivity and transmission of a probe pulse are measured for time delays extending over several probe pulse lengths. The relatively constant values will indicate the suitability of the ideal plasma slab approximation as explained above. Additional support

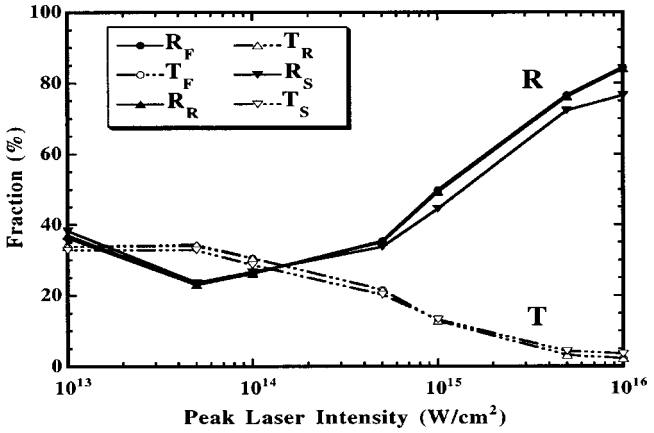

FIG. 2. Reflectivity and transmission calculated from full hydrodynamic simulations $\{R_F, T_F\}$and $\{R_R, T_R\}$for front- or rear-side probes and $\{R_S, T_S\}$ with the slab approximation.

can be obtained from symmetry considerations by comparing the reflectivity and transmission of the front- and rear-side probes at the end of the pump pulse. The method for further data reduction is illustrated in Fig. 3. We begin by using the measured reflectivity R_F^*(or R_R^*) and transmission T_F^* (or T_R^*) of a front-side (or rear-side) probe pulse in the electromagnetic wave solver routine to solve for the dielectric function of the slab plasma, which also yields the ac conductivity, $\sigma_{S\omega}$. To determine the condition of the idealized slab plasma, we will use the measured values of reflectivity R^* and transmission T^* of the pump laser pulse. These yield the energy deposited in the foil and using the QEOS, we can calculate the electron density and temperature of the slab plasma, which is assumed to remain at normal solid density. This procedure thus leads to a direct measurement of the ac conductivity at a specific electron density and temperature. If the conductivity model for the plasma of interest is known, it can then be used to calculate an ac conductivity σ_ω for comparison with $\sigma_{S\omega}$.

To simulate this procedure, we will adopt results of our full hydrodynamic calculations presented above. That is, $\{R^*, T^*\}$ are replaced with $\{R, T\}$ while $\{R_F^*, T_F^*\}$ (or $\{R_R^*, T_R^*\}$) are replaced with $(R_F, T_F\}$ (or $\{R_R, T_R\}$). A comparison of the corresponding σ_ω and $\sigma_{S\omega}$ is presented in Figs. 4(a) and 4(b). Figure 4(c) shows the corresponding electron densities. The close agreement is not a test of the validity of our plasma conductivity model since the hypothetical experimental data used are obtained from simulations based on the same transport model. Rather, such an agreement demonstrates the validity of the idealized slab plasma approximation and illustrates the feasibility of obtaining experimental ac conductivity data for very dense plasmas.

In an experiment, the accuracy in determining n_e and T_e of the idealized slab plasma will depend on that of the

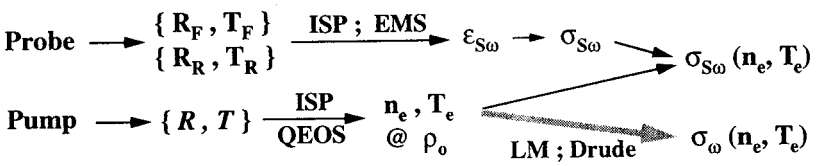

FIG. 3. Method for data reduction in a pump-probe measurement. EMS, electromagnetic wave solver; ISP, idealized slab plasma; QEOS, quotidian equation of state; LM, Lee-More conductivity.

$\{R^*,T^*\}$ values for the pump pulse. Uncertainties in the measured $\{R_F^*,T_F^*\}$ or $\{R_R^*,T_R^*\}$values for the probe will lead to uncertainties in the derived values of $\sigma_{S\omega}$. To test such sensitivities, we evaluate the maximum errors, assuming that all reflectivity and transmission measurements can be made with $\pm 10\%$ or $\pm 5\%$ relative accuracies. The corresponding error bars are illustrated in Figs. 4(a) and 4(b).

As stated earlier, our calculations assume equilibrium conditions. Limited by available theoretical models, we can only assess nonequilibrium effects in an isolated and non-self-consistent manner. For fs laser heating, electrons gain energy directly from the laser field and the ions lag in temperature. Calculations have been made using a two-temperature prescription of the QEOS while electron-ion equilibration is treated in a relaxation model with a free, coupling parameter [19]. Even for an electron-ion equilibration rate three orders of magnitude below the Brysk value [20], the results show minor differences from that obtained for the equilibrium plasma. We also test our calculations using a two-temperature plasma conductivity model of Perrot and Dharma-wardana [21], which assumes an ion temperature fixed to the lattice melting point. This shows little effect. Furthermore, calculations have been made using ionization determined from a collisional-radiative-equilibrium or a time-dependent collisional-radiative model. The effect of nonequilibrium ionization is minimal. This might be attributed to the large collision frequencies characteristic of the dense and relatively cold plasma of interest.

As a sensitivity test, calculations have also been made for 20-fs pump and probe pulses with a broader wing structure similar to that of an experimental 120-fs, 1-ω pulse [4]. The results show that the idealized slab plasma approximation remains valid and the ac conductivity can be measured as better than 35%. If the durations of the 2-ω pump and probe laser pulses were increased to 30 fs, the accuracy of the ac conductivity measurement would deteriorate to about 60% at the highest pump irradiance of 10^{16} W/cm^2. On the other hand, if an aluminum foil of 200 Å were used with the 20-fs, 2ω pump and probe pulses, the ac conductivity can be deter-

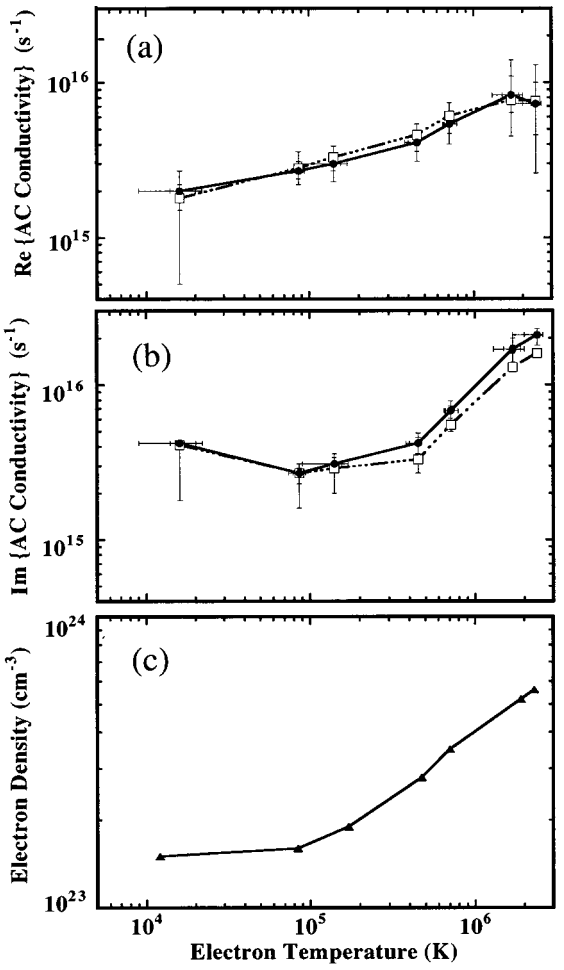

FIG. 4. Comparison of the (a) real and (b) imaginary part of the ac conductivity derived with the idealized slab plasma approximation (solid circles) to the corresponding values (open squares) obtained from the Lee-More conductivity model. Uncertainties in the conductivities correspond to $\pm 10\%$ or $\pm 5\%$ relative accuracies in reflectivity and transmission; the larger error bars are associated with the poorer accuracies. The corresponding electron density of the idealized plasma slab is given in (c).

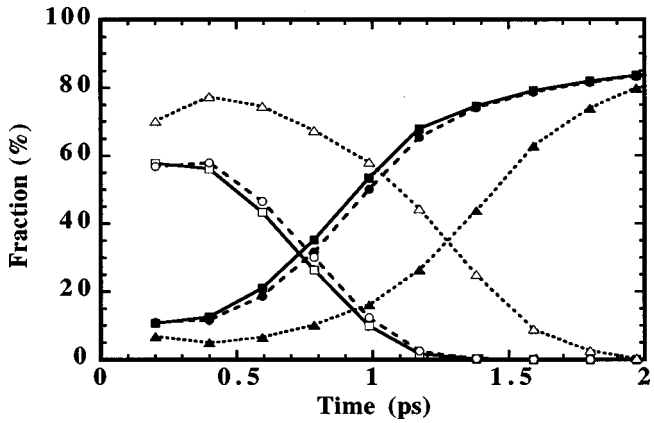

FIG. 5. Reflectivity *(R)* and transmission *(T)* of a time-delayed probe for results obtained from full hydrodynamic simulations using the QEOS and the Lee-More conductivity model (open and solid circles) or idealized slab plasma approximation (open and solid squares), and for results of full hydrodynamic simulations using the Sesame equation of state and Rinker's conductivity (open and solid triangles).

mined to within 25% accuracy.

In addition to allowing the measurement of ac conductivity in the strongly coupled regime, the idealized slab plasma can also serve as an initial value problem for studying hot expanded states. Once the slab plasma is produced at the end of the pump pulse, it undergoes free expansion from a well-defined initial state. The significance of an initial value problem approach is that the initial plasma conditions can be determined from the absorbed energy and an equation of state, avoiding the need to accurately calculate the interaction of the pump pulse with the target. By extending the time delay of the probe pulse, the reflectivity and transmission of the probe can be used to test models describing hot expanded states. As an example, we present results of a calculation for a 100-Å aluminum foil heated with a 20-fs (FWHM), 400-nm, pump pulse incident normally at 10^{15} W/cm^2. As the slab expands, the reflectivity and transmission of a 20-fs (FWHM), 260-nm probe laser incident normally on the target rear side can be calculated with our LTC-EMS code using an initial condition either (a) the plasma density and temperature profiles derived from full hydrodynamic simulation of the heating of the foil by the pump pulse or (b) the idealized slab plasma density and temperature derived from the absorbed pump laser energy and equation of state. As shown in Fig. 5, such calculations incorporating the QEOS and LM's conductivities are essentially identical, supporting the treatment of the expanding plasma as an initial value problem. Results of full hydrodynamic simulation using the Sesame data for equation of state [22] and Rinker's conductivities [23] are also presented in Fig. 5. The difference between these and the results using the QEOS and the Lee-More conductivity model is striking and readily measurable. This offers an opportunity to test our theoretical understanding of hot expanded states. At the present time, we cannot decouple conductivity from the equation of state because the Lee-More conductivity model utilizes the ionization from the QEOS, whereas Rinker's conductivity uses the Sesame ionization.

In conclusion, we have illustrated an approach of using intense fs lasers and ultrathin foils to produce idealized slab plasmas of uniform electron density and temperature, allowing direct measurements of the ac conductivity of strongly coupled plasmas. The ac conductivity can be analyzed to provide information about the electron mean-free path in the low temperature regime and the ionization state in the high temperature regime. In addition, fs-laser heated ultrathin foils can be used to produce a well-defined plasma in an initial value problem description for probing hot expanded states of matter.

[1] H. M. Milchberg, R. R. Freeman, S. C. Davey, and R. M. More, Phys. Rev. Lett. **61**, 2364 (1988).

[2] R. Fedosejevs, R. Ottmann, R. Sigel, G. Kuhnle, S. Szatmari, and F. P. Schafer, Phys. Rev. Lett. **64**, 1250 (1990).

[3] A. Ng, P. Celliers, A. Forsman, R. M. More, Y. T. Lee, F. Perrot, M. W. C. Dharma-wardana, and G. A. Rinker, Phys. Rev. Lett. **72**, 3351 (1994).

[4] D. F. Price, R. M. More, R. S. Walling, G. Guethlein, R. L. Shepherd, R. E. Stewart, and W. E. White, Phys. Rev. Lett. **75**, 252 (1995).

[5] G. Guethlein, M. E. Foord, and D. Price, Phys. Rev. Lett. **77**, 1055 (1996).

[6] B. T. Vu, A. Szoke, and O. L. Landen, Phys. Rev. Lett. **72**, 3823 (1994).

[7] A. Ng and A. Forsman, Phys. Rev. E **51**, R5208 (1995).

[8] J. A. Cobble, G. A. Kyrala, A. A. Hauer, A. J. Taylor, C. C. Gomez, N. D. Delamater, and G. T. Schappert, Phys. Rev. A **39**, 454 (1989).

[9] M. M. Murnane, H. C. Kapteyn, and R. W. Falcone, Phys. Rev. Lett. **62**, 155 (1989).

[10] Z. Jiang, J. C. Kieffer, J. P. Matte, M. Chaker, O. Peyrusse, D. Gilles, G. Korn, A. Maksimchuk, S. Coe, and G. Mourou, Phys. Plasmas **2**, 1702 (1995).

[11] O. Peyrusse, M. Busquet, J. C. Kieffer, Z. Jiang, and C. Y. Cote, Phys. Rev. Lett. **75**, 3862 (1995).

[12] R. C. Mancini, A. S. Shlyaptseva, P. Auderbert, J. P. Geindre, S. Bastiani, J. C. Gauthier, G. Grillon, A. Mysyrowicz, and A. Antonetti, Phys. Rev. E **54**, 4147 (1996).

[13] U. Teubner, I. Uschmann, P. Gibbon, D. Altenbernd, E. Forster, T. Feurer, W. Theobald, R. Sauerbrey, G. Hirst, M. H. Key, J. Lister, and D. Neely, Phys. Rev. E **54**, 4167 (1996).

[14] R. Evans, A. D. Badger, F. Fallies, M. Mahdieh, T. A. Hall, P. Auderbert, J. P. Geindre, J. C. Gauthier, A. Mysyrowicz, G. Grillon, and A. Antonetti, Phys. Rev. Lett. **77**, 3359 (1996).

[15] D. H. Reitze, H. Ahn, and M. C. Downer, Phys. Rev. B **45**, 2677 (1992).

[16] P. Celliers and A. Ng, Phys. Rev. E **47**, 3547 (1993).

[17] R. M. More, K. H. Warren, D. A. Young, and G. B. Zimmerman, Phys. Fluids **31**, 3059 (1988).

[18] Y. T. Lee and R. M. More, Phys. Fluids **27**, 1273 (1984).

[19] A. Ng, P. Celliers, G. Xu, and A. Forsman, Phys. Rev. E **52**, 4299 (1995).

[20] H. Brysk, Plasma Phys. **16**, 927 (1974).

[21] F. Perrot and M. W. C. Dharma-wardana (private communication).

[22] K. S. Holian, Los Alamos National Laboratory Report No. LA-10160-MS UC-34, 1984 (unpublished).

[23] G. A. Rinker, Phys. Rev. B **31**, 4207 (1985); **31**, 4220 (1985).